

Article

Foam Concrete Produced with Recycled Concrete Powder and Phase Change Materials

Osman Gencel ^{1,*}, Mehrab Nodehi ², Gökhan Hekimoğlu ³, Abid Ustaoglu ⁴, Ahmet Sari ^{3,5}, Gökhan Kaplan ⁶, Oguzhan Yavuz Bayraktar ⁷, Mucahit Sutcu ⁸ and Togay Ozbakkaloglu ^{2,*}

¹ Civil Engineering Department, Faculty of Engineering, Architecture and Design, Bartın University, 74100 Bartın, Turkey

² Ingram School of Engineering, Texas State University, San Marcos, TX 78666, USA; mehrab1nodehi@gmail.com

³ Department of Metallurgical and Material Engineering, Karadeniz Technical University, 61080 Trabzon, Turkey; ghekimoglu@ktu.edu.tr (G.H.); ahmet.sari@ktu.edu.tr (A.S.)

⁴ Department of Mechanical Engineering, Faculty of Engineering, Architecture and Design, Bartın University, 74100 Bartın, Turkey; abidusta@gmail.com

⁵ Centers of Research Excellence, Renewable Energy Research Institute, King Fahd University of Petroleum and Minerals, Dhahran 31261, Saudi Arabia

⁶ Civil Engineering Department, Ataturk University, 25030 Erzurum, Turkey; gkaplan@atauni.edu.tr

⁷ Civil Engineering Department, Kastamonu University, 37150 Kastamonu, Turkey; obayraktar@kastamonu.edu.tr

⁸ Department of Materials Science and Engineering, Izmir Katip Celebi University, 35620 Izmir, Turkey; mucahit.sutcu@ikc.edu.tr

* Correspondence: ogenel@bartin.edu.tr (O.G.); togay.oz@txstate.edu (T.O.)



Citation: Gencel, O.; Nodehi, M.; Hekimoğlu, G.; Ustaoglu, A.; Sari, A.; Kaplan, G.; Bayraktar, O.Y.; Sutcu, M.; Ozbakkaloglu, T. Foam Concrete Produced with Recycled Concrete Powder and Phase Change Materials. *Sustainability* **2022**, *14*, 7458. <https://doi.org/10.3390/su14127458>

Academic Editors: Jorge de Brito and Miguel Bravo

Received: 2 June 2022

Accepted: 16 June 2022

Published: 18 June 2022

Publisher's Note: MDPI stays neutral with regard to jurisdictional claims in published maps and institutional affiliations.



Copyright: © 2022 by the authors. Licensee MDPI, Basel, Switzerland. This article is an open access article distributed under the terms and conditions of the Creative Commons Attribution (CC BY) license (<https://creativecommons.org/licenses/by/4.0/>).

Abstract: In construction industry, phase change materials (PCMs), have recently been studied and found effective in increasing energy efficiency of buildings through their high capacity to store thermal energy. In this study, a combination of Capric (CA)-Palmitic acid (PA) with optimum mass ratio of 85–15% is used and impregnated with recycled concrete powder (RCP). The resulting composite is produced as foam concrete and tested for a series of physico-mechanical, thermal and microstructural properties. The results show that recycled concrete powder can host PCMs without leaking if used in proper quantity. Further, the differential scanning calorimetry (DSC) results show that the produced RCP/CA-PA composites have a latent heat capacity of 34.1 and 33.5 J/g in liquid and solid phases, respectively, which is found to remain stable even after 300 phase changing cycles. In this regard, the indoor temperature performance of the rooms supplied with composite foams made with PCMs, showed significantly enhanced efficiency. In addition, it is shown that inclusion of PCMs in foam concrete can significantly reduce porosity and pore connectivity, resulting in enhanced mechanical properties. The results are found promising and point to the suitability of using RCP-impregnated PCMs in foam composites to enhance thermo-regulative performance of buildings. On this basis, the use of PCMs for enhanced thermal properties of buildings are recommended, especially to be used in conjunction with foam concrete.

Keywords: recycled concrete powder; phase change materials; foam concrete; capric and palmitic acid; thermal energy storage

1. Introduction

Starting from the early 20th century and the industrial revolution, an increasing trend of urbanization took place that continues to this date. According to the World Bank [1], currently, over 55% of the world's population (~4.2 billion inhabitants) live in urban areas while this value is projected to be increased by 1.5 times until 2045 and reach a total of 6 billion people. Although such scale of urban sprawl require major resource challenges, it is estimated to be also responsible for over 70% of the total greenhouse gas production

and consume some 75% of global energy supply [2]. The U.S. Energy Information Administration (EIA) [3], estimates that about 30% of the total energy consumption of urban areas is directly used in buildings, mostly for cooling and heating purposes. To address this and follow sustainable means, recent advances in construction and building materials have attempted increasing the energy efficiency of buildings by utilizing highly porous composite materials that have a lower thermal conductivity [4–6]. This includes a series of lightweight composite materials, such as lightweight and foam concretes produced through open-graded aggregates, porous aggregates, or a foaming agent [7,8].

Although porous composites are known to be energy efficient, their rate of energy retention is known to be considerably low [9], since they only reduce the conductivity of materials and are not a mean to store thermal energy. This leads to inefficient use of energy for temperature control in buildings. As a result, recent studies have reported that the use of novel phase change materials (PCMs) can increase the energy retention rate significantly [10] through their considerable capacity to retain thermal energy while changing their phases.

In general, PCMs refer to specific class of organic or inorganic compounds that have a low melting temperature and high latent heat of fusion [11] that gives them the ability to absorb and release a large amount of thermal energy, as they change phase [12]. This can be melting (or liquifying) and resolidifying, in case of solid-liquid PCMs, but it can also be merely softening or hardening in case of solid-solid PCMs [13]. Nonetheless, due to certain volume change and other elemental impracticality, not all forms of PCMs can be used for construction purposes [13]. In this sense, according to Ref. [11], the selection of proper PCMs for successful use in buildings depends on various thermodynamic, chemical and economic criteria.

In general, recent studies (e.g., [14]) have reported that fatty acid-based PCMs can be very suitable for thermal energy (or heat) storage applications due to their outstanding properties, such as cost effectiveness, high capacity for latent heat storage, thermal reliability, non-toxicity, low vapor pressure in the liquid phase, as well as negligible supercooling and high stability [15]. Nonetheless, since the melting and resolidifying temperature point of the mentioned pure PCMs are constant, using a combination of PCMs can provide further tailoring-ability to adjust the mentioned temperature points as needed, by using a mixed ratio of multiple PCMs [15]. According to Refs. [16–18], eutectic mixture of Capric (CA)-Palmitic acid (PA) can be used for this purpose due to their relatively high compatibility and proper performance for indoor thermoregulation in buildings. As reported by Ref. [19], unlike certain organic PCMs, a combination of CA-PA does not produce separate freezing (or solidifying points), making the two an ideal group of PCMs to be used as composite.

Although organic PCMs have numerous benefits, they are known to be prone to leakage, and thus, requiring a specific packaging method, such as impregnation [20], micro-encapsulation [21], and adsorption [22]. In either case, however, impregnating PCMs into a highly porous media, such as foam concrete, can be an effective way to avoid leakage, especially as the porous medium can adsorb the PCMs through capillary force and surface tension [19]. To provide such conditions, this study adopted the use of recycled concrete powder which is known to be a solid waste material and have relatively high internal porosity [23]. It is reported that concrete powder originating from construction and demolition (C&D) has an annual production of about 600 million tons, only in the United States [24], and is considered as a solid waste material. Nevertheless, waste concrete powder is commonly considered as an inferior material for reuse, as a recycled construction material due to its high porosity and weak interfacial transition zone (ITZ) with other aggregates, resulting in reduced physico-mechanical properties [25,26].

Nonetheless, its use in foam concrete have been recently practiced (e.g., [26,27]) and often found beneficial since it generally reduces pore connectivity and settlement tendency of foams while it does not significantly increase the conductivity of the produced foams since it is a porous byproduct [23,28,29]. In general, foam concrete refers to a class of lightweight concrete with significantly reduced density and very high degree of porosity [6,8,30,31]

that has major uses as insulating composite materials. Nonetheless, it is known that foams are incapable of retaining a considerable amount of thermal energy and its use is merely for insulation purposes.

To date, however, no study has used recycled concrete powder to be impregnated by PCMs in foam concrete. Ref. [32], for instance, utilized expanded clay, as lightweight aggregates to micro-encapsulate paraffin but had to polymer coat the aggregates to avoid leakage. Similarly, Ref. [33] impregnated paraffin into expanded clay and pumice and reported that such combination can increase the life span of bridge and the major infrastructure by at least a few years due to its high effectiveness in reducing the adverse effect of freeze thawing. However, the mentioned study again used porous aggregates as a means to host PCMs and did not provide further information on the leakage of the produced materials, neither studied the actual thermal properties of the produced cementitious composites. In addition, Ref. [34] impregnated paraffin into diatomite and reported a maximum latent heat absorption of 70.51 J/g. Similar set of materials have also been used by Ref. [35] and reported that up to 67% of the PCM has been leaked when impregnated into diatomite, suggesting alternative means for the impregnation of PCMs. Similarly, Hunger et al. [36] used waste marble powder as encapsulating agent of paraffin and reported the optimum rate of paraffin inclusion is 3% from which the physico-mechanical properties are significantly impacted. Other studies (e.g., [37,38]), impregnated PCMs similarly in porous media and reported enhanced thermal retention of the produced concretes, as well as documenting certain leakage shortcoming.

As can be seen in the above literature review, although various techniques have been used to suitably incorporate PCMs in concrete, to date, no attempt has been done to use recycled concrete powder as a means for storing a combination of CA-PA. This combination can lead to enhanced thermo-physical properties, as compared to ordinary foams and other studies. Similarly, since the inclusion of recycled concrete powder is reported to lower the pore connectivity [39–41], this can also avoid PCMs leakage problems. As a result, this study, for the first time, studied the impregnation of a mixed combination of PCMs into recycled concrete powder, since recycled concrete powder has the ability to adsorb and host PCMs in liquid form. To suitably evaluate the properties of the produced samples, a series of physico-mechanical, thermal and microstructural tests have been conducted and reported. Additionally, specifically designed tests have been carried out to evaluate a detailed thermal performance of the produced samples. Further information, regarding the methodology of this research can be found in the following sections.

2. Methodology and Materials

2.1. Materials

2.1.1. Cement

In this study, CEM I Portland cement with specific surface area of 3346 (cm²/g) and a CaO content of ~61.9% has been used. Further information on the physicochemical properties of the used Portland cement can be found in Table 1.

2.1.2. Foam Agent

In this study, Sodium lauryl sulfate (SLS)-based foaming agent with a pH of ~8.8 and a specific gravity of around 100 g/L has been used. SLS is known to be an anionic surfactant that is heavily used in industrial foam production. In this study, SLS has been added to the water in a ratio of 95:5 water to SLS by weight. Followed by this, the foam was obtained by mixing with a high-speed mixer, and was then added to the cementitious materials. The reason for choosing such method is the authors extensive previous experience with foam concretes ensuring that no aggregate settlement or bubble instability takes place [6,8].

Table 1. Chemical and physical properties of CEM I 42.5 R Cement.

Oxide	%	Physical Properties	
CaO	61.9	Specific gravity	3.15
SiO ₂	20.2	Specific surface area (cm ² /g)	3346
Al ₂ O ₃	4.8	Volume stability (mm)	0.3
Fe ₂ O ₃	4.3	Initial setting time (mm)	175
MgO	1.8	Final setting time (mm)	265
Na ₂ O	0.5	2-days compressive strength (MPa)	15.2
K ₂ O	0.6	28-days compressive strength (MPa)	46.2
SO ₃	3.2		
LOI	2.5		

2.1.3. Waste Concrete Powder

In this research, waste concrete powder with a specific gravity of 2.58 and a particle size of <0.25 mm has been used. To produce the concrete powder, it was first obtained from the debris landfill of the municipality. Waste concrete was separated from the debris in the field and brought to the laboratory. Firstly, the waste concrete was prepared in fine aggregate size (4 mm) with a laboratory crusher. Afterwards, it was ground into powder form with a ball mill where it was grinded for 1 h and sieved through 0.250 mm sieve size and was later impregnated with PCMs. The compressive strength of the waste concrete in the field is low and its contents are not known exactly. However, according to the XRD pattern, it is thought to contain limestone-based aggregates. Also, the chemical composition of the produced waste concrete powder can be seen in Table 2. Also, as presented in Figure 1, a significant quartz peak was observed in the waste concrete powder. In addition, Ca-based anorthite and portlandite peaks can also be seen. These peaks are believed to have been caused by the cement content, left in the recycled concrete. In addition, the calcite peak representing CaCO₃ can also be determined. The calcite peak is believed to have formed due to carbonation in the concrete.

Table 2. Chemical composition of the waste concrete powder.

CaO	SiO ₂	Al ₂ O ₃	Fe ₂ O ₃	MgO	SO ₃	Na ₂ O _(eq)	LOI
37.3	29.8	6.4	3.2	2.1	0.6	1.8	18.3

2.1.4. Silica Sand

In this study, silica sand with a maximum particle size of 2 mm and a water absorption of ~2.1% has been used. Further information on the properties of the silica sand can be found in Table 3. Figure 1 also presents the XRD of silica sand where the quartz peaks were observed. It is also notable that the silica sand used had a SiO₂ content of more than 95%.

Table 3. Silica sand properties.

Specific Gravity	Particle Size (mm)	Water Absorption (%)	Color
2.69	0–2	2.1	Light yellow

2.1.5. PCMs

In this study, a combination of capric acid (CA) with a purity degree of ≥98.0%, and palmitic acid (PA) with an overall purity degree of ≥99.0% were supplied from Merck Inc. Darmstadt, Germany, used. Figure 2 presents the XRD result of the combined PCMs. Based on the figure, the peaks occurring at 11.4, 21.4 and 23.5° are resulted due to crystallization.

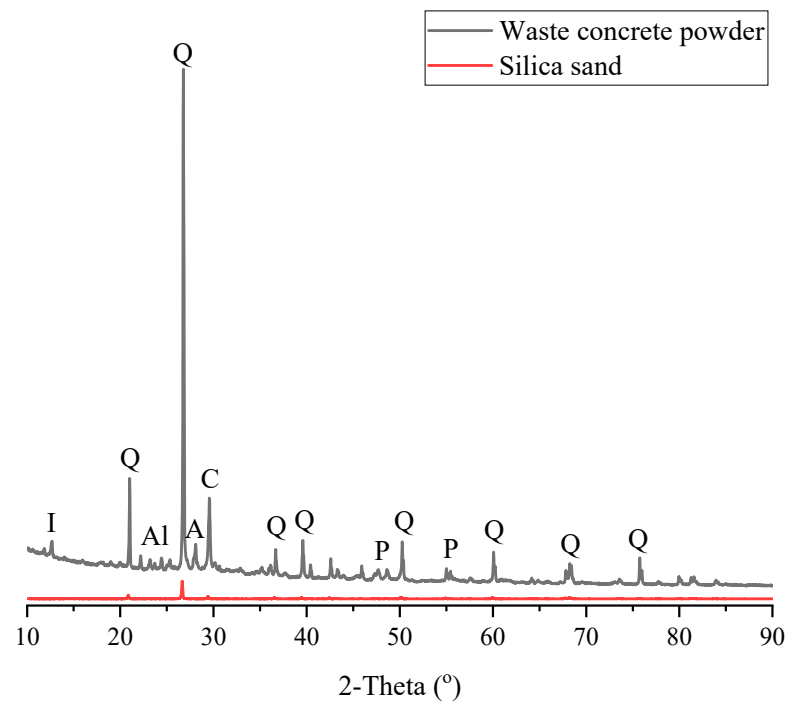


Figure 1. XRD pattern of waste concrete powder and silica sand (I: illite, Q: quartz, Al: albite, A: anorthite, C: calcite, P: portlandite).

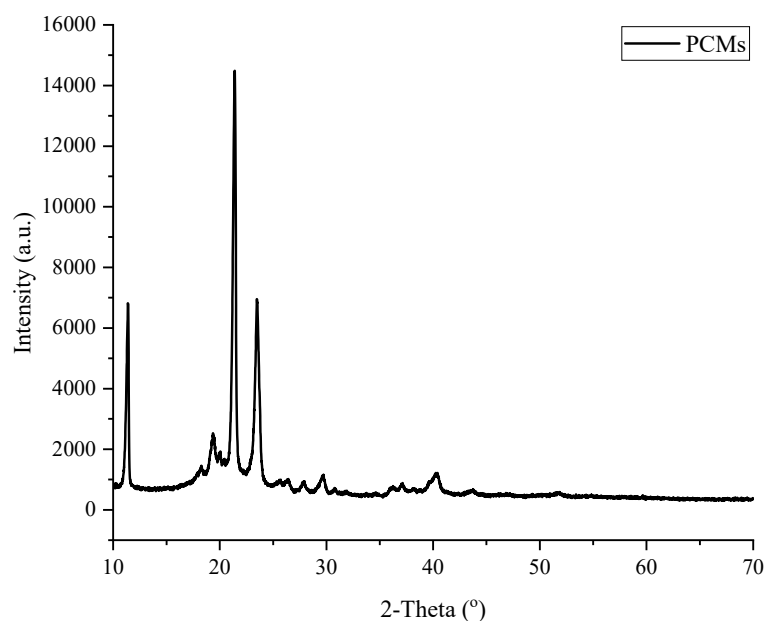


Figure 2. XRD pattern of PCMs.

2.2. Preparation of Form-Stable Recycled Concrete Powder (RCP)/PCM Composite

Initially, a CA-PA eutectic mixture utilized as PCM was prepared, and the optimum mass ratios of the two PCMs used was 85–15%, as recommended by Refs. [42,43]. As in Ref. [16], then, a stable form of RCP/PCM composite was produced by using vacuum impregnation method. In doing so, certain content of RCP was mixed with melted CA-PA in beakers. The mixes were then put in vacuum oven at 60 °C for 2 h. Following the vacuum operation, the RCP/PCM mixtures were removed from oven and left for cooling in ambient temperature until they became ready for stability performance test. In this way, the stability of the composite materials was evaluated by monitoring the leakage tendency

during the phase transition. In this assessment, various ranges of RCP/PCM mixtures were prepared with different CA-PA contents, ranging from 10–40 wt%. The results showed that the highest possible CA-PA rate in the recycled concrete powder that does not leak the PCMs is around 20 wt% of the recycled-concrete-powder's weight, as shown from Figure 3.

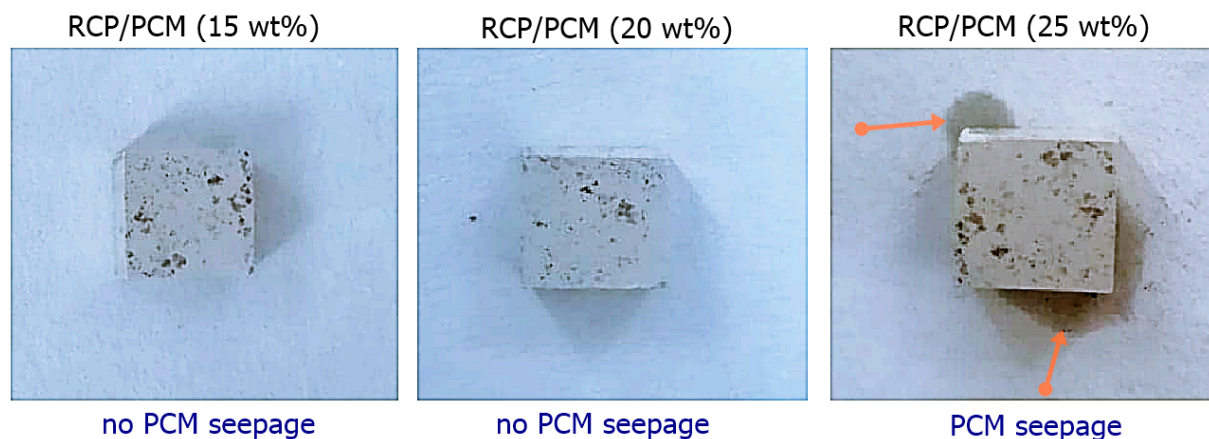


Figure 3. Form stability test results of RCP/PCM composites produced with different CA-PA ratio.

2.3. Specimen Preparation for Testing

In this study, cement and water have been firstly mixed for about 1 min. Then, silica sand and waste concrete powder were added to the mix and the mix continued for another 2 min where the foaming agent was added to the mixture. The total mixing took about 5 min. The produced samples were then molded and stored under laboratory conditions for 24 h. Followed by this, foam concretes were removed from their molds and subjected to water curing until the testing day. The physical properties of the mixtures were measured after 28 days of water curing. Table 4 presents the testing method, standard and sample sizes used in this study while Table 5 provides information about the mixing proportions.

Table 4. Presenting the testing method, standard and sample sizes used in this study.

Test Method	Standard	Sample Size (mm)
Water absorption-Porosity	ASTM C 642 [44]	50 × 50 × 50
Flexural strength	ASTM C 348 [45]	40 × 40 × 160
Compressive strength	ASTM C 349 [46]	40 × 40 × 160
Unit weight	ASTM C138 [47]	–
Capillary water absorption	EN 1015-18 [48]	50 × 50 × 50

Table 5. Materials proportion in each mix (kg/m³).

Material	Mix-1	Mix-2	Mix-3
Cement	300	300	300
Water	150	150	150
Foam	75	75	75
Silica Sand	700	–	–
RCP	–	667	–
RCP-PCM	–	–	667

2.4. Characterization

The thermal capacity of the pure CA-PA and RCP/PCM composites were evaluated by utilizing a Differential Scanning Calorimeter (DSC, HITACHI 7020 model) at a constant heating/cooling rate of 3 °C/min, and under a 30 mL/min of nitrogen gas atmosphere.

2.5. Thermal Performance

To evaluate the thermal energy performance of the produced foams, three identical test fixtures or small-sized rooms were produced by using medium density fiberboard (MDF) with a thickness of 0.02 m, as in Ref. [49]. To induce the actual building conditions, a two-layered glazed window with a dimension of $0.14 \times 0.14 \times 0.02$ m with a solar radiation transmissivity of 0.77 were attached to the top of the fixtures. In addition, the inner walls of the MDFs were surrounded by expanded polystyrene (EPS) foam with a thickness of 0.05 m size. The foam mortar specimens were placed on the floor of the fixtures. Finally, the fixtures were placed on the rooftop of a building with a coordinate of $41^{\circ}38'8.99''$ N and $32^{\circ}2'15''$ E. To evaluate the actual solar radiation inside of the fixtures, Eco MS-410 first class pyranometer has been used, as shown in Figure 4. Further, the temperatures within and outside of the fixtures were measured by using T-type thermocouples, connected to a 10-channel Graphtec data logger that recorded temperature and radiation data, as shown in Figure 4.



Figure 4. Experimental setup and thermocouple positions on the test cabins (28 April 2022).

3. Results

3.1. DSC Analysis

Figure 5 presents the results of DSC thermograms of pure CA-PA and CA-PA impregnated RCP/PCM composite. Based on the curve of CA-PA, the peaks clearly show the accuracy of the eutectic mixture ratio of 85–15 wt% representing the expected phase transformations at proper temperatures. Based on Figure 5, the start of the liquefying (or melting) and solidifying (or freezing) temperatures of CA-PA are found to be at 21.63 and 20.78 °C, respectively. Similarly, when the CA-PA are impregnated into RCP, the resulting composite has a melting and solidifying temperatures of 21.62 and 19.75 °C, respectively. Further, the latent heat of CA-PA in liquifying and solidifying phase change processes are also determined as 172 and 170 J/g, respectively. When the CA-PA is impregnated into RCP, however, these values change to be 34.1 and 33.5 J/g, respectively. This value is considerably close to the theoretical latent heat capacity that can be calculated through multiplication of the latent heat capacity of pure PCM with the impregnation ratio in the composite. This results in theoretical melting and solidification latent heat values of 34.4 J/g and 34.1 J/g for the RCP/PCM, respectively. Further from Figure 5, the DSC curves of RCP/PCM composite before and after 300 thermal cycling tests are compared and presented. Based on these curves, the composite does not show a particular change in the trends and the resulted latent heat of RCP/PCM is measured as 33.8 and 33.3 J/g, respectively. This shows a very small variation as a result of 300 liquifying and solidifying that confirms the stability of the produced RCP/PCM composite.

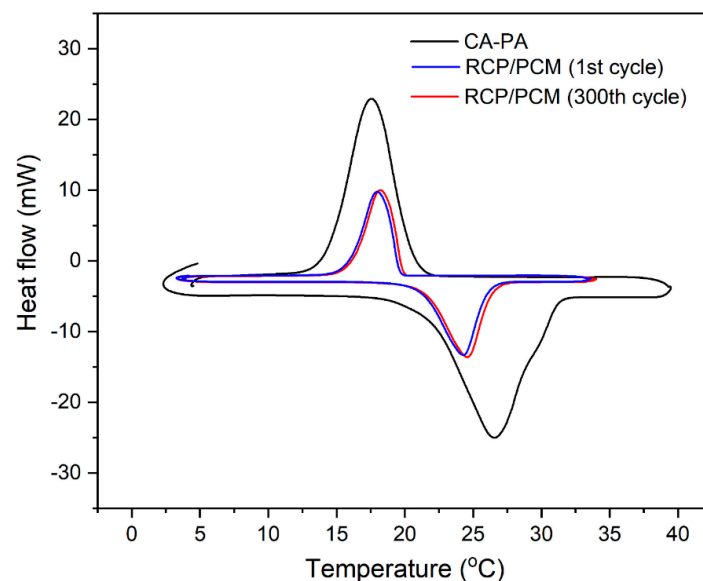


Figure 5. The DSC curve of CA-PA and form-stable RCP/PCM (20 wt%) composite (before and after 300 melting-freezing cycles).

3.2. Unit Weight

Figure 6 presents the result of unit weight of various samples. Based on this figure, the inclusion of recycled concrete powder has increased the unit weight value by ~11%. This increase can be associated with filling effect of concrete powder. Refs [50–52] also reported higher compaction due to the inclusion of the concrete powder. Further, the inclusion of PCM in recycled concrete powder has increased the unit weight values by about 44%, despite the similar overall volume of materials used in the Mix-3 versus Mix-1. This significant rise in the unit weight value can be due to the higher specific gravity of the PCMs used in this study that fills in the pores leading to higher unit weight values. Similar results are reported in Ref. [53] that utilized polyethylene glycol, impregnated into lightweight aggregates and achieved up to 9% increased unit weight values.

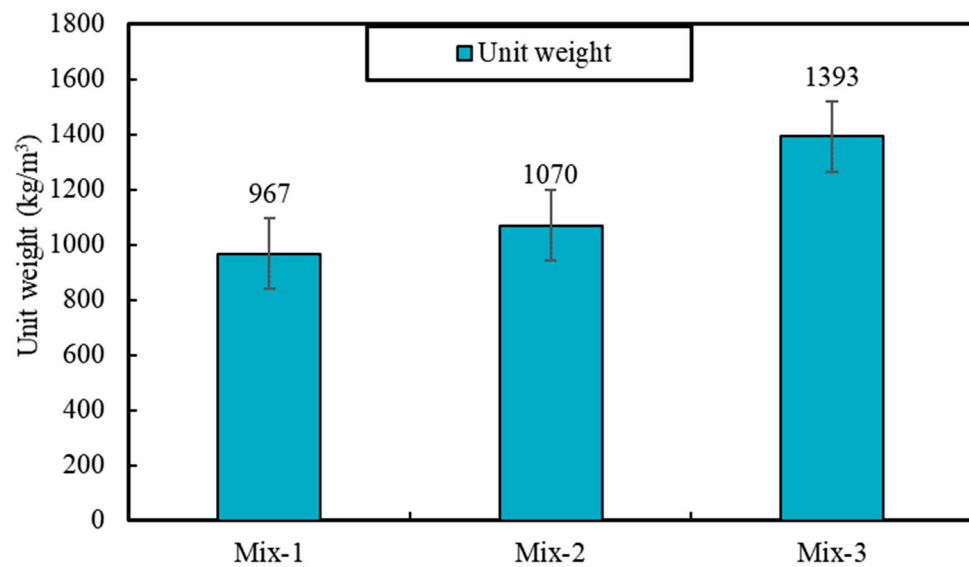


Figure 6. Unit weight of various mixes.

3.3. Apparent Porosity

Apparent porosity is a means to evaluate the pore content of cementitious foams and its potential in hosting free water [8]. The result of apparent porosity test is presented in Figure 7. Based on this, the inclusion of recycled concrete powder is found not to have a considerable impact on the porosity values. Most notably, the results indicate a ~6% reduction of porosity values when compared to the mix produced with silica sand. The reason for this can be the high porosity of recycled concrete powder that can host or even channel micro pores, despite their filling effect on air-void pores. Ref. [54] used scanning electron microscopy (SEM) images and showed that that recycled concrete powder generally has a porosity of above 1% in its microstructure and thus, does not significantly reduce the overall porosity of the produced concretes. Nonetheless and from Figure 7, when PCM are impregnated to the recycled concrete powder, significant reduction of porosity, about ~32%, takes place. This further confirms the high impact of PCM in reducing the content of micropores and their respective connectivity.

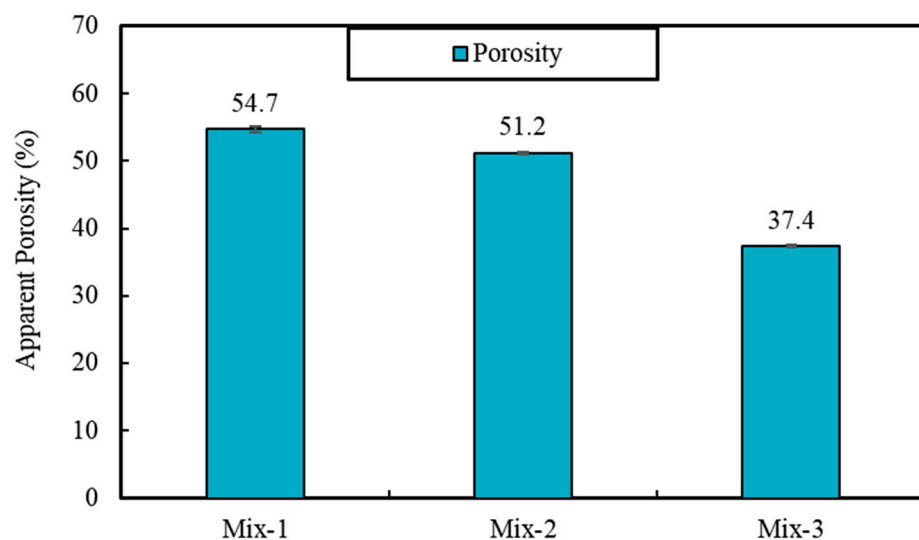


Figure 7. Apparent porosity of various mixes.

3.4. Water Absorption

Water absorption test conducted in this study after 28 days of curing the materials and is presented in Figure 8a. As can be seen, the highest and lowest water absorption rate is for Mix-1 produced with silica sand with 32.3% and mix-3 produced with recycled concrete powder, impregnated with PCM with 21.9%, respectively. This shows that the inclusion of recycled concrete powder did not have significant impact on the water absorption (by only reducing it ~8%). This is aligned with the results outlined in Section 3.2 and point to the inherent porosity of recycled concrete powder. Similar results are reported in literature extensively [55,56]. However, when PCM are impregnated to the recycled concrete powder, a 32% reduction is observed. This reduction is aligned with the results of porosity reported in Section 3.2 and shows the filling effect of PCM on micropores. Ref. [57] utilized organic PCM (polyethylene glycol), and reported its considerable compatibility in filling micropores and cracks of hardened concrete. Similarly, Bi et al. [58], used paraffin as PCM and reported significant reduction of water absorption and associated it with the improvement of hydrophobic characteristics in the pores when PCM are used. This can be better seen in Figure 8b that shows capillary water absorption. In general, capillary water absorption shows the transport mechanism of water in micro pores through surface interaction of water and the pore wall [59]. Based on this figure, the impregnation of PCM has reduced the capillary water absorption by ~360%. This result further confirms that the inclusion of PCM alters the hydrophobic characteristics of the produced foams, considerably.

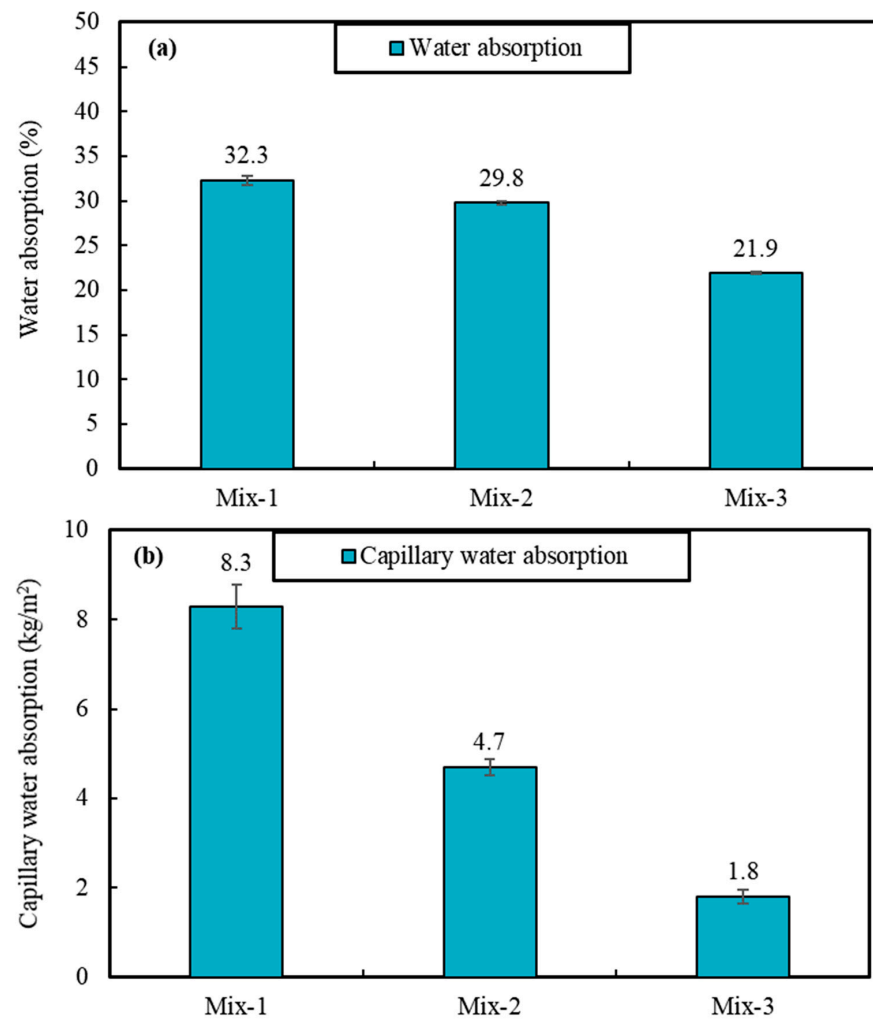


Figure 8. (a) Water absorption and (b) capillary water absorption of various mixes.

3.5. Compressive Strength

The result of compressive strength test conducted after 7 and 28 days of curing is presented in Figure 9. As can be seen, the inclusion of recycled concrete powder has only increased the compressive strength for ~37% and 15% for 7 and 28 day cured specimens, respectively. This higher strength development shows that the effect of recycled concrete powder is mostly the filling of pores, as was also reported in Ref. [60]. Despite this moderate increase in compressive strength values, when PCM are used ~397% and 204% increase in compressive strength results are achieved for specimens cured for 7 and 28 days, respectively. Such significant improvement in compressive strength values can be associated with the change in rheological properties of mixes containing PCMs coupled with their filling of micropores within the recycled concrete powder. According to Ref. [61] when PCM with hydrophilic surface are used, the rheology and particle distribution of the produced samples tend to be affected significantly and lead to a more homogenous particle distribution, as well as a reduction of segregation. This would then lead to enhanced mechanical properties as shown in Figure 9.

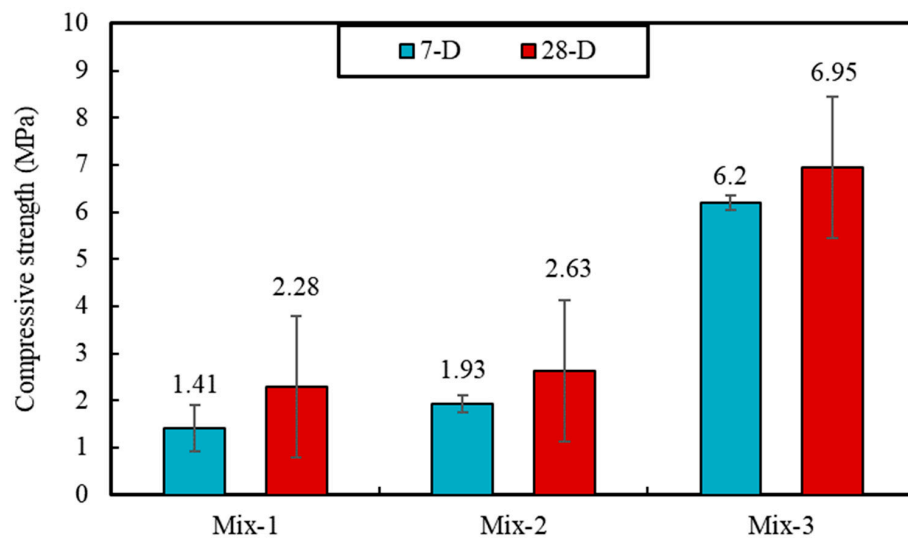


Figure 9. Compressive strength of various mixes.

3.6. Flexural Strength

Figure 10, presents the result of flexural strength conducted after 7 and 28 days of curing. Based on the figure, the inclusion of recycled concrete powder has increased the flexural strength values by ~24% and 15%, after 7 and 28 days of curing, respectively. Similar to the compressive strength results, outlined in Section 3.4, the inclusion of PCM impregnated recycled concrete powder increases the flexural strength values by 224% and 108%, at 7 and 28 days of curing, respectively. As discussed in previous section, the inclusion of recycled concrete powder does not improve the strength values significantly, due to its inherent porosity. Nonetheless, when the PCMs are impregnated in its pores, the strength values increase considerably. Similar results are reported in Ref. [53] that impregnated polyethylene glycol into lightweight aggregates and reported up to 17% increase in the flexural strength values.

3.7. Thermal Conductivity

Thermal conductivity is a means to evaluate the rate of thermal conduction of a given material and its insulating properties [62,63]. Figure 11 presents the result of thermal conductivity test conducted on specimens cured for 28 days. Based on this figure, the inclusion of recycled concrete powder has had a positive impact (about 4.5% increase) on the conductivity value, despite the slightly lowered apparent porosity reported in Section 3.2. The reason for this can be the impact of micro pores within the recycled

concrete powder and reduction of pore connectivity. As reported in Ref. [64], a closed cell-foam can have a considerably lower conductivity values since it does not allow heat loss from its pores. Nonetheless, when PCM are impregnated to the recycled powder, 43% increase in conductivity values are documented. This is aligned with the results of water absorption and porosity values that point to the filling of micro pores when PCMs are impregnated in the recycled fine concrete powder.

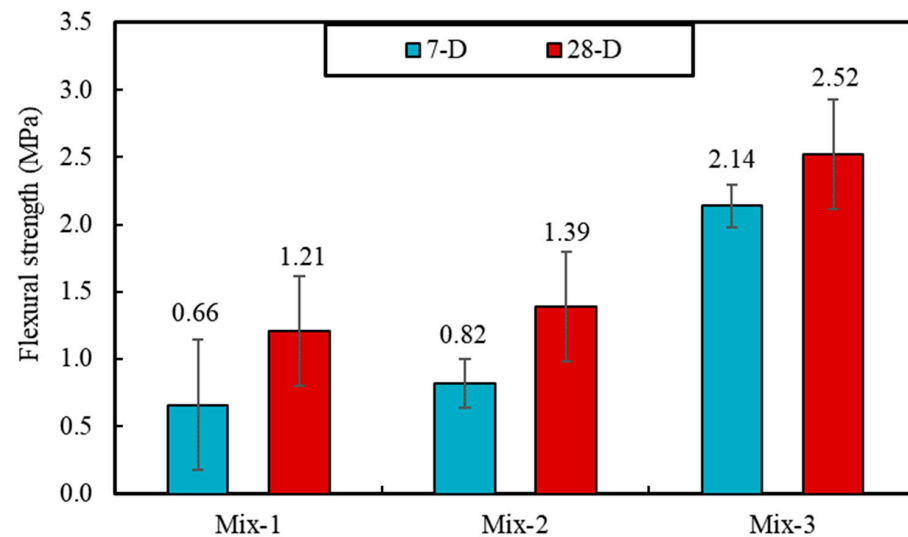


Figure 10. Flexural strength of various mixes.

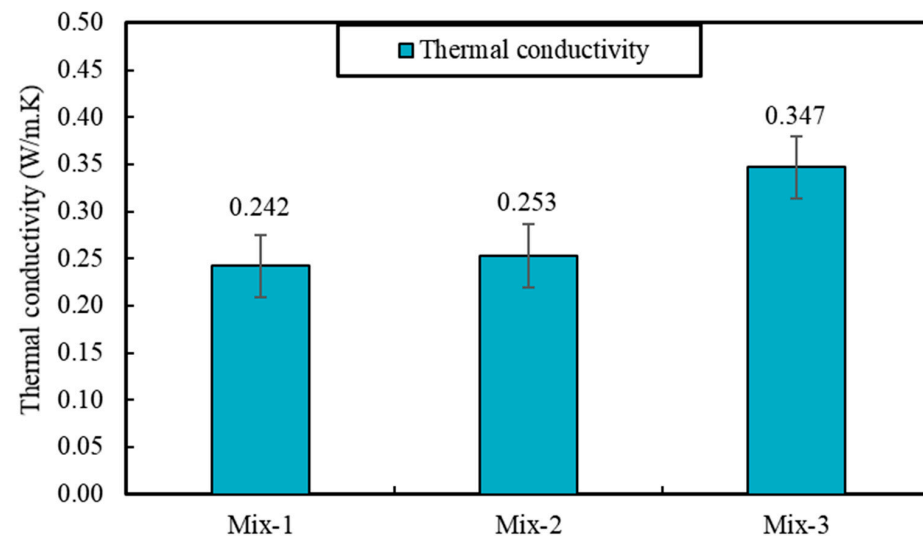
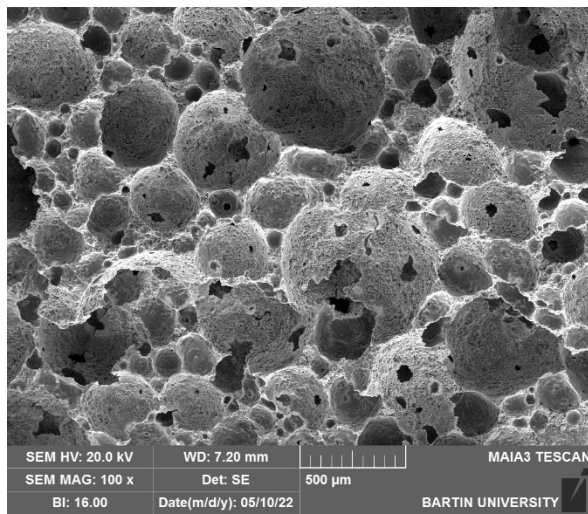


Figure 11. Thermal conductivity of various mixes.

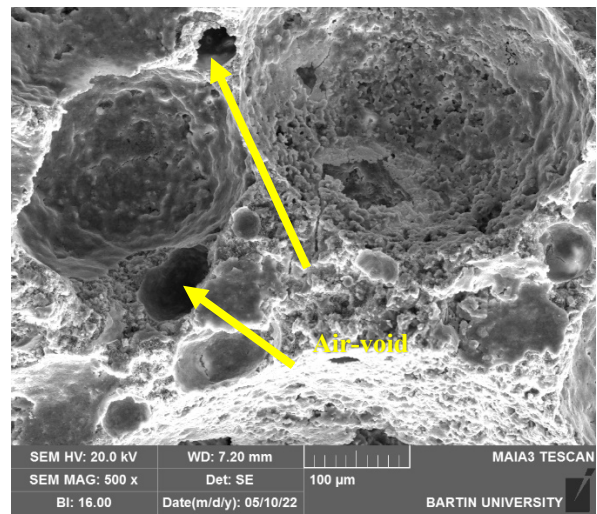
3.8. Microstructural Properties

3.8.1. SEM

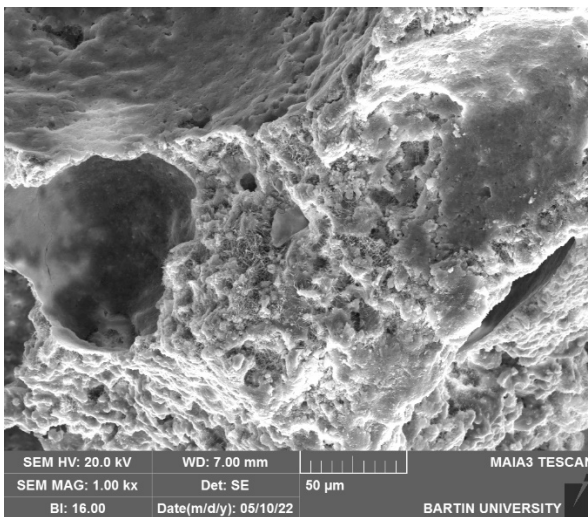
Figure 12a–l present the results of SEM images taken from the 28-day cured specimens. Based on Figure 12a–d, the pores produced in foams of Mix-1 are found to be relatively deep and often interconnected. In Figure 12e–h, however, the overall content of pores is found to have slightly lowered but a high content of unconnected particles can be seen which represents a weak interfacial transition zone (ITZ) for Mix-2 produced with recycled concrete powder. Figure 12i–l, however, shows that the inclusion of PCMs has significantly changed the pore types of the foamed samples by making them highly disconnected. The mentioned results further confirm the results achieved in Sections 3.2, 3.3 and 3.6.



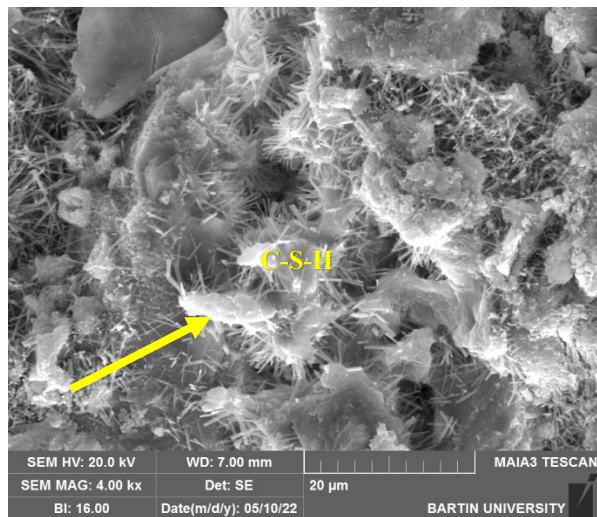
(a)



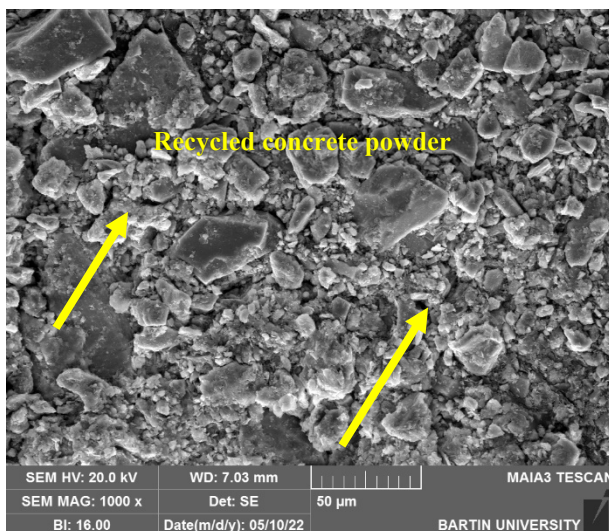
(b)



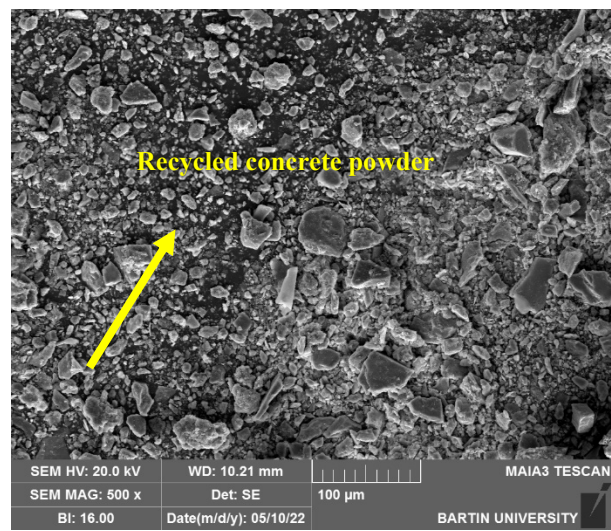
(c)



(d)

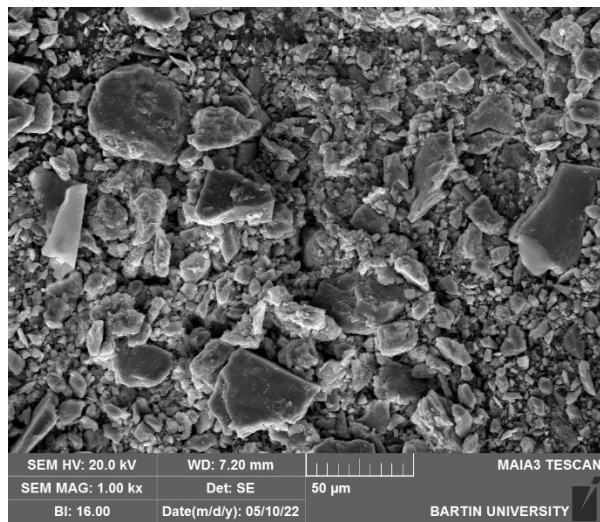


(e)

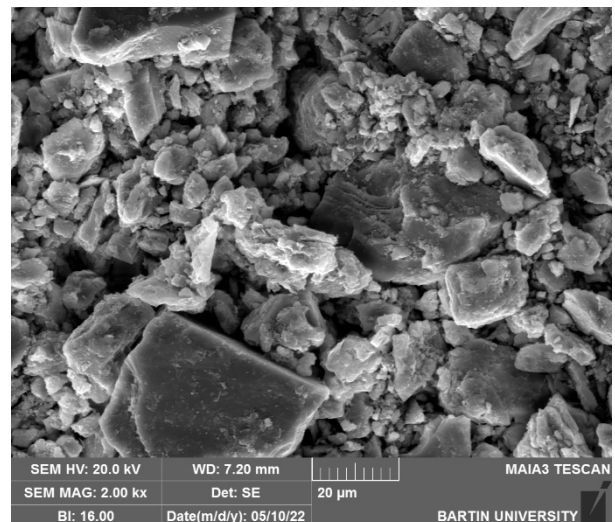


(f)

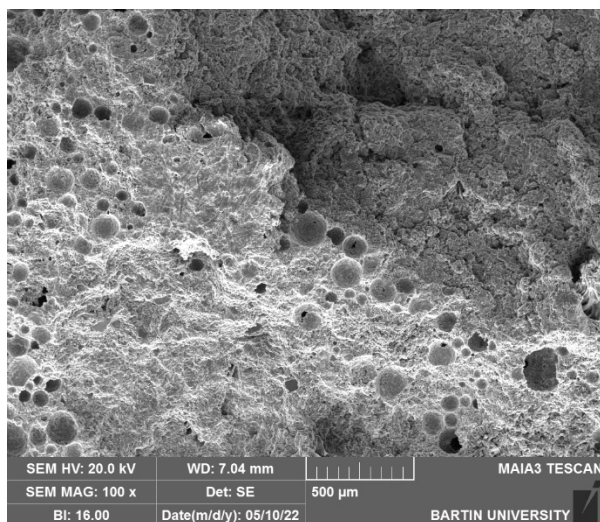
Figure 12. Cont.



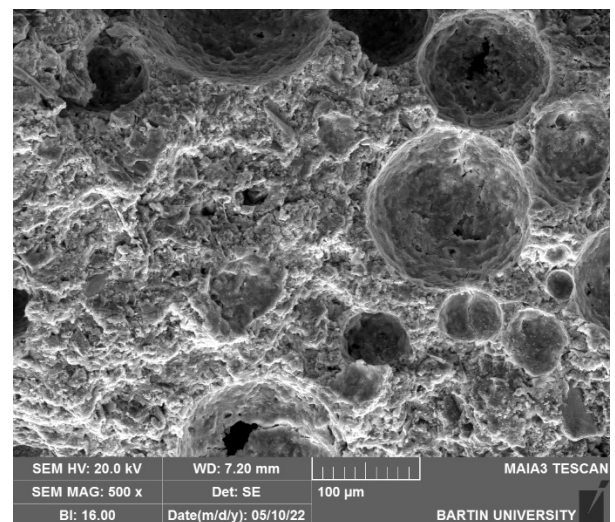
(g)



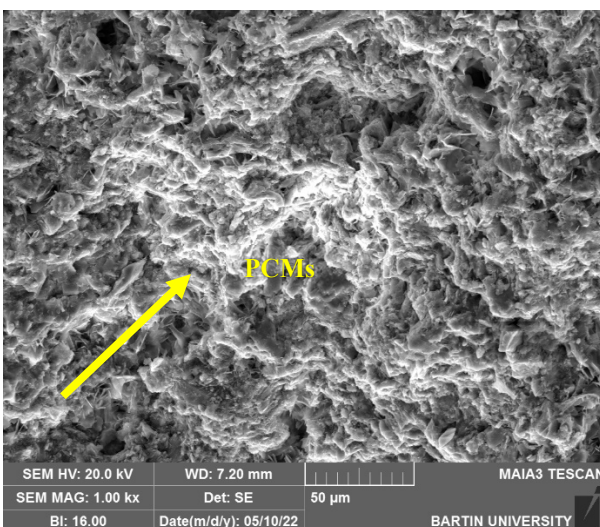
(h)



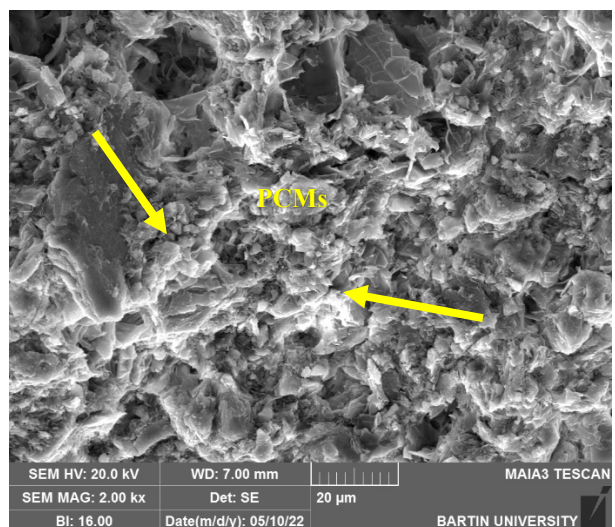
(i)



(j)



(k)



(l)

Figure 12. SEM images of mixes at various scales. (a–d) Mix-1, (e–h) Mix-2, (i–l) Mix-3.

3.8.2. EDS

The EDS results of various mixes is presented in Table 6. As can be seen in this table, the average compositional values of Mix-1 have the highest Ca and the lowest C content. In turn, Mix-2 samples have the highest C and lowest Ca content. The reason for this can be the carbonation of the produced samples, as also noted in Section 2.1.3, as well as the old cementitious paste resulting in high content of C and Ca, that are further discussed by Refs. [65,66]. When PCMs are impregnated, however, the Ca, C and Si content is found to shift toward Mix-1 with increased content of C. Similarly, Ref. [43] conducted EDS on pure CA-PA composite and reported a high content of C and O atoms. These observations are aligned with what has been reported in Section 3.8.1 that more similarity is seen between the Mix-1 and Mix-3.

Table 6. The chemical composition of various samples produced from mixes.

Mix No.	Ca	C	Si	Fe	S	Al	Mg
Mix-1.1	73.6	0	11.9	5.3	3.8	3.9	1.5
Mix-1.1	76.9	0	13.4	3.5	2.9	2.3	1
Mix-1.1	87.6	0	4.7	7.7	0	0	0
Mix-1.1	84.3	0	5.6	8.8	0	1.3	0
Mix-1.2	79.4	0	7.6	4.7	5.3	3	0
Mix-1.2	74	0	9.6	5.1	5.9	4	1.4
Mix-1.2	76.5	0	19.4	1.4	0	1.1	1.6
Mix-1.2	56.9	0	18.7	9.2	11.5	3.7	0
Average	76.15	0	11.36	5.71	3.60	2.41	0.68
Mix-2.1	39	56.7	3.1	0	0	0.7	0.5
Mix-2.1	37.6	55.6	5.3	0	0	0.8	0
Mix-2.1	6.4	68.8	17.4	0	0	4.6	0
Mix-2.1	40.4	51.4	5.2	0.8	0	1.4	0.7
Mix-2.2	16.4	0	53.8	0	0	23.7	0
Mix-2.2	21.9	63.5	9.3	0	0	2.6	0.5
Mix-2.2	29	52.2	17.2	0	0	1	0
Mix-2.2	5.5	58.9	13	9.6	0	3.6	2.8
Average	24.52	50.88	15.53	1.30	0	4.80	0.56
Mix-3.1	69.9	0	17.6	3.6	2.4	4.4	2.1
Mix-3.1	80.8	0	11.7	3.9	1.8	1.8	0
Mix-3.1	98.2	0	1.8	0	0	0	0
Mix-3.1	70.8	0	15.2	5.1	2.9	4.2	1.9
Mix-3.2	22.9	74	2.4	0	0	0.7	0
Mix-3.2	70.6	0	16.1	2.7	4.9	4.7	1
Mix-3.2	76.1	0	14.3	3.8	1.7	2.3	1.9
Mix-3.2	70.8	0	11.4	6.4	6.6	4.8	0
Mix-3.3	47.5	51.2	1.3	0	0	0	0
Mix-3.3	62.3	0	12.1	13.5	2.3	3.6	6.1
Mix-3.3	98	0	2	0	0	0	0
Mix-3.3	70.3	0	21.6	2.9	1.3	2.4	1.5
Mix-3.4	13	70.3	15.8	0	0	0.5	0
Mix-3.4	16.8	74	5.9	0	0	1.6	0.3
Mix-3.4	24.7	0	62.3	1.2	0	2.4	0
Mix-3.4	66.9	0	23.5	2	0	3.6	1.3
Mix-3.5	47.9	45.8	5.1	0	0	0	0
Mix-3.5	29.8	55.4	13.2	0	0	0.6	0
Mix-3.5	9.9	64.7	15.6	0	0	5.4	0.5
Mix-3.5	22.6	62.2	9.4	2.1	0	1.4	0.7
Average	53.49	24.88	13.91	2.36	1.19	2.22	0.86

3.9. Thermal Energy Storage Performance

Figure 13 presents the result of global, direct and diffuse solar irradiation on the surface of the produced fixtures from 6:00 morning to 20:00 evening of the location that produced rooms and samples have been tested for their energy storage performance. In general, global radiation presents the total radiation that reaches the horizontal surface of the measured samples. In turn, unlike direct radiation that directly reaches the samples' surface, diffuse radiation is part of the total radiation that reaches the surface of fixture after being scattered by the surrounding environments [67,68]. Based on the figure, it is notable that the diffuse radiation is dependent on the sky clearness and has changed as the clearness changed in the coordinate of $41^{\circ}38'8.99''$ N and $32^{\circ}2'15''$ E on 23 February 2022 and a cloudy-sunny sky. Further from this figure, it can be seen that the global and direct radiation values are at their peaks at around 9:40–15:00, as the radiation level is at its highest during this time period.

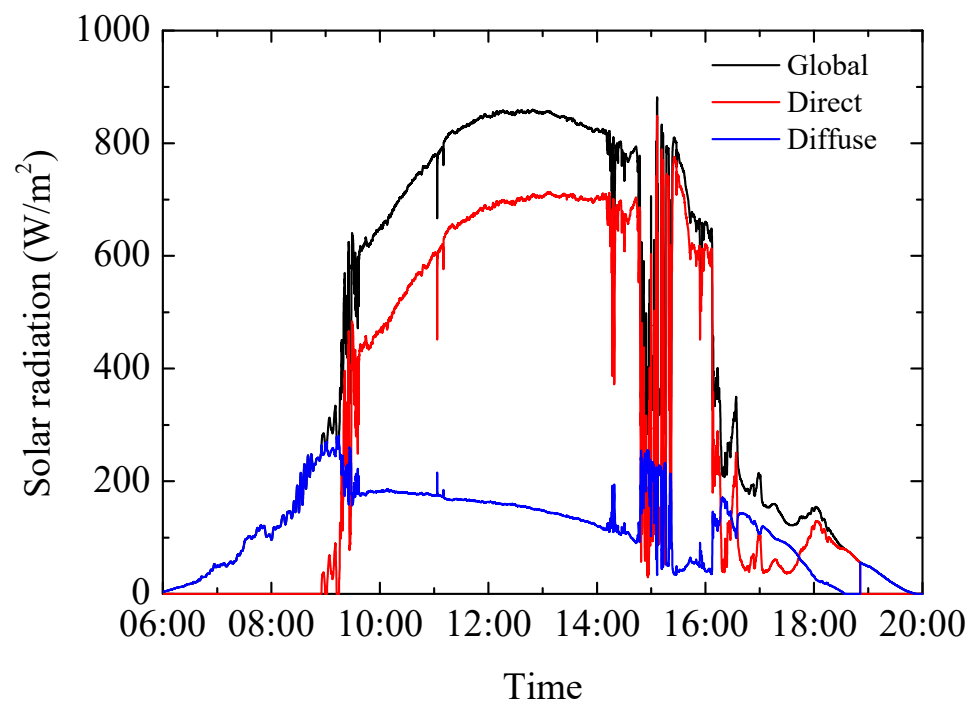


Figure 13. Global, direct, and diffuse solar radiation data on 23 February 2022 cloudy-sunny sky.

Figure 14 shows the temperature change in the prepared fixtures as measured by the thermocouples. As noted in the figure, TCp1 through TCp8 were placed in various parts of the fixtures and TCp9 refers to the reference ambient temperature. Based on the figure, at around 14:00 when the temperature of the room center becomes the highest, the lower surface of the fixture that the produced foams are located, have a considerably lower temperature. After around 15:00, however, the lower surface can be seen to have kept a higher temperature.

Figure 15a,b show the average temperature differences of reference sample (a) and the one containing PCMs. As can be seen, at various times, the temperature is about a few minutes to a few hours away from the reference sample. This helps reducing the peaks and can also be associated with the absorption and desorption of heat by PCMs which is found to be very effective in reducing the peak temperatures and potentially increasing the energy efficiency of the sample rooms.

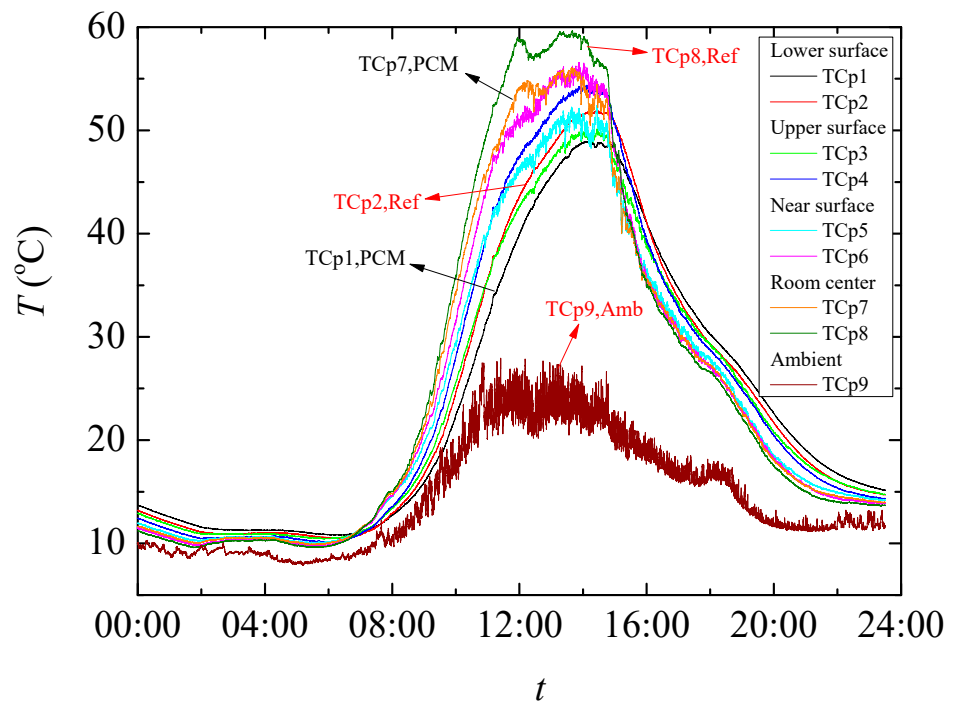


Figure 14. Temperature variations in the test room and reference rooms on 28 April 2022 cloudy-sunny sky.

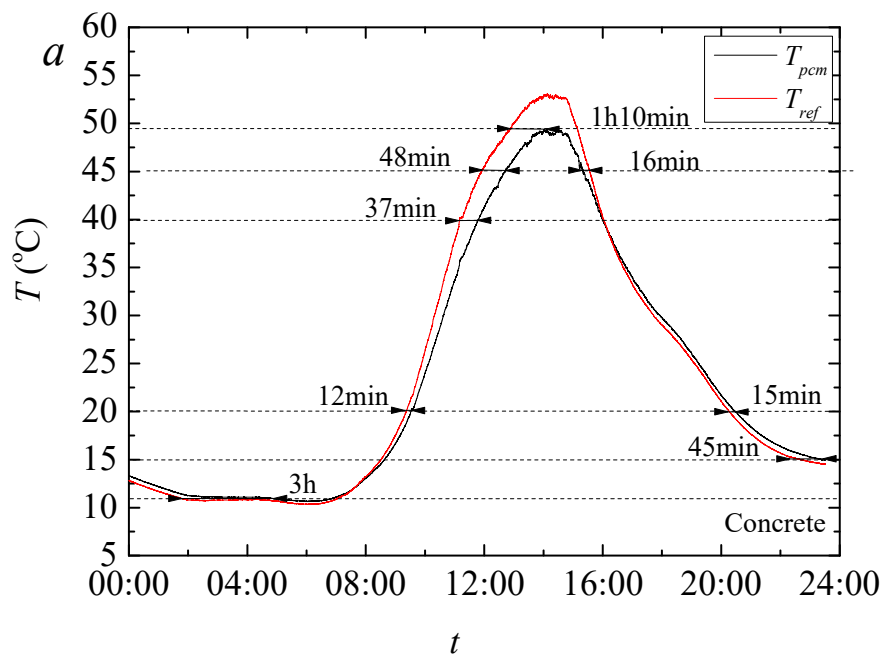


Figure 15. Cont.

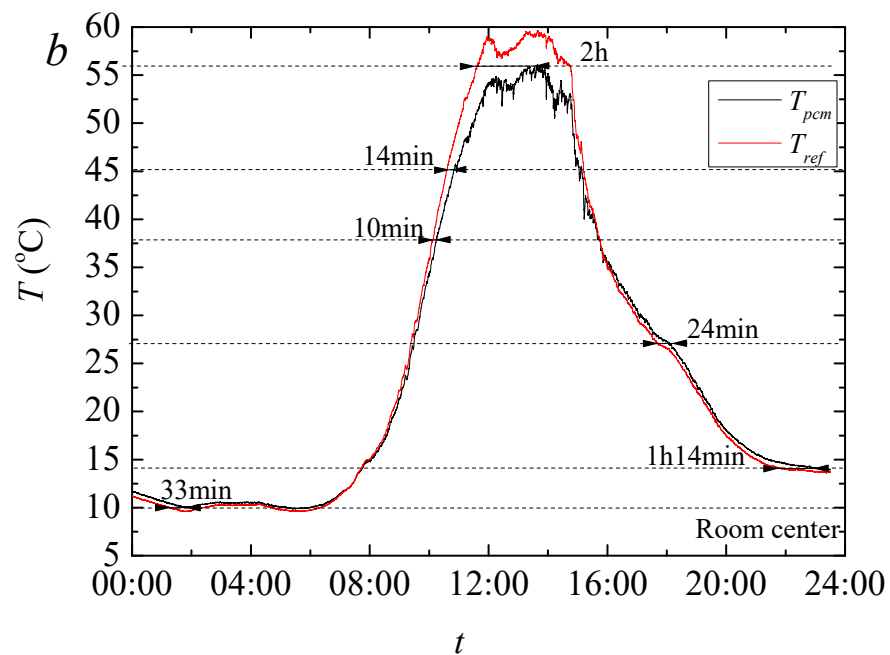


Figure 15. Temperature variation for waste concrete (a) and room center (b) on 28 April 2022 cloudy-sunny sky.

Figure 16 shows the temperature difference between the reference versus PCM containing samples between the lower and upper surface (a), as well as near surface and room center (b). Based on Figure 16a, the upper surface of the sample containing PCMs is found to have $-5.07\text{ }^{\circ}\text{C}$ lower temperature at peak daytime temperature. In turn, at evening time, up to $3.67\text{ }^{\circ}\text{C}$ higher temperature is recorded. Similar results can be seen for lower surface all of which point to the enhanced energy retention of samples when $T_{\text{PCM}} - T_{\text{ref}}$ is calculated.

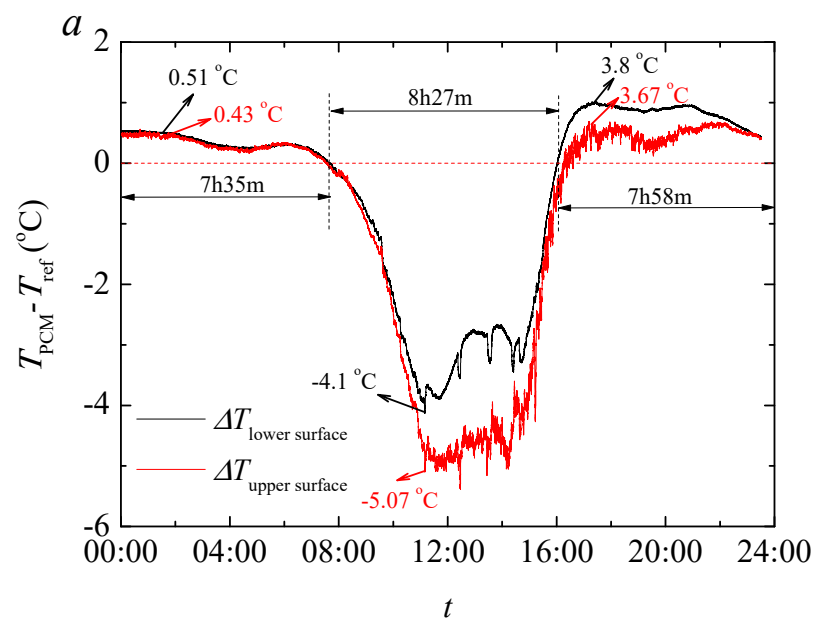


Figure 16. Cont.

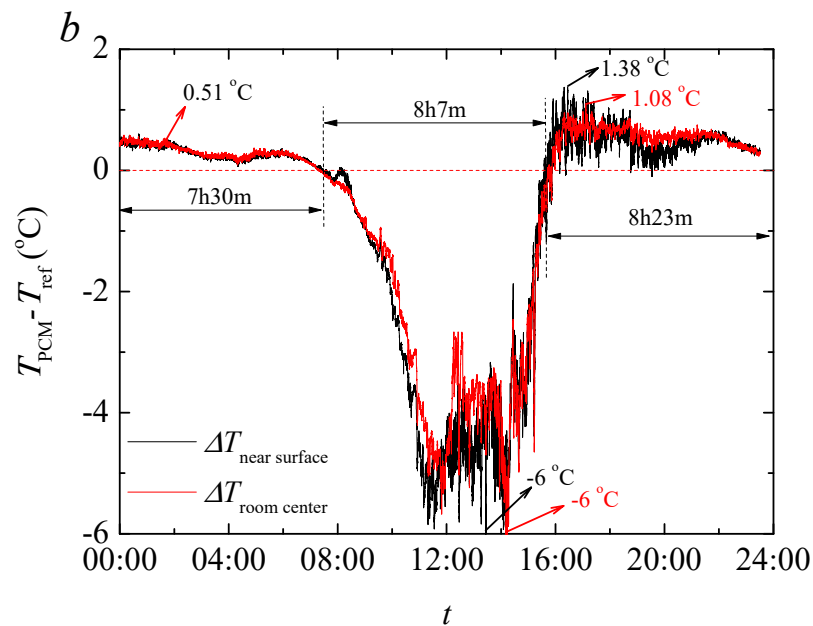


Figure 16. Temperature difference between PCM-WCON and WCON for lower and upper surfaces (a) and temperature difference between PCM-WCON and WCON for near surfaces and room centers (b) on 28 April 2022 cloudy-sunny.

Figure 17 shows the temperature difference between concrete and the ambient temperature, as well as between the room centers and the ambient temperature around fixtures. As can be seen, the foam sample produced with PCMs is found to have absorbed the highest thermal energy until around 15:00, at around 32 °C that compares to reference sample of 27 °C. From that point, it starts to discharge the heat, and thus, sustains lower temperature in itself. Similarly, the room center temperature when the ambient temperature is at its peak is considerably lower (e.g., 34.7 °C versus 38.5 °C). Similar to the concrete temperatures, after around 15:00, it starts to discharge the absorbed heat and maintain a higher temperature. Further, it is notable that the mentioned variation in energy values is for the small-sized sample rooms produced for this study which can potentially be further pronounced in larger scale applications.

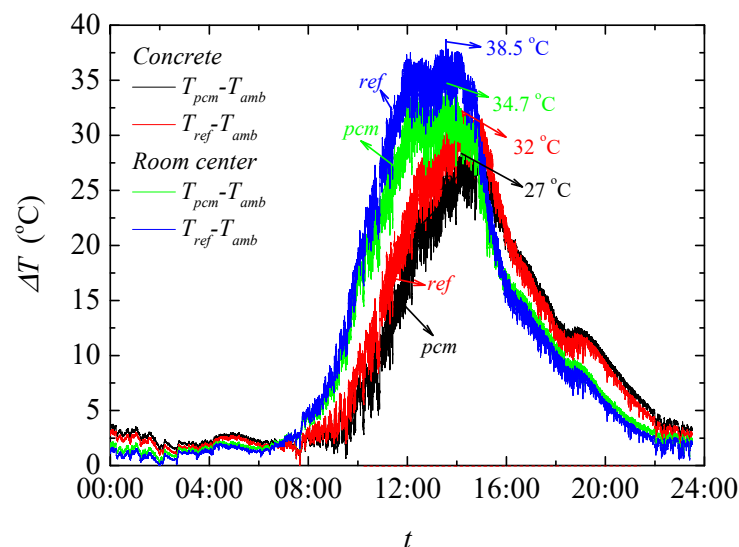


Figure 17. Temperature difference between concretes and ambient; and between room centers and ambient on 28 April 2022 sunny sky.

Figure 18 presents the result of thermal camera conducted on the produced rooms at various hours. As can be seen, at 11:17 morning, even the surface temperature of the room containing foam with PCMs (FCRCP-PCM) is 1.3–2.2 °C lower than the room containing ordinary foam and recycled concrete powder (FCRCP). Similarly, and as the time passes until 13:47, this change is seen to be relatively similar and range from 0.1–1.7 °C. The reason for this slightly lower performance at later hours can be the mentioned shift in the peak temperatures that causes the internal temperature to be considerably enhanced by the inclusion of PCMs. Similar results have been reported by Ref. [69].

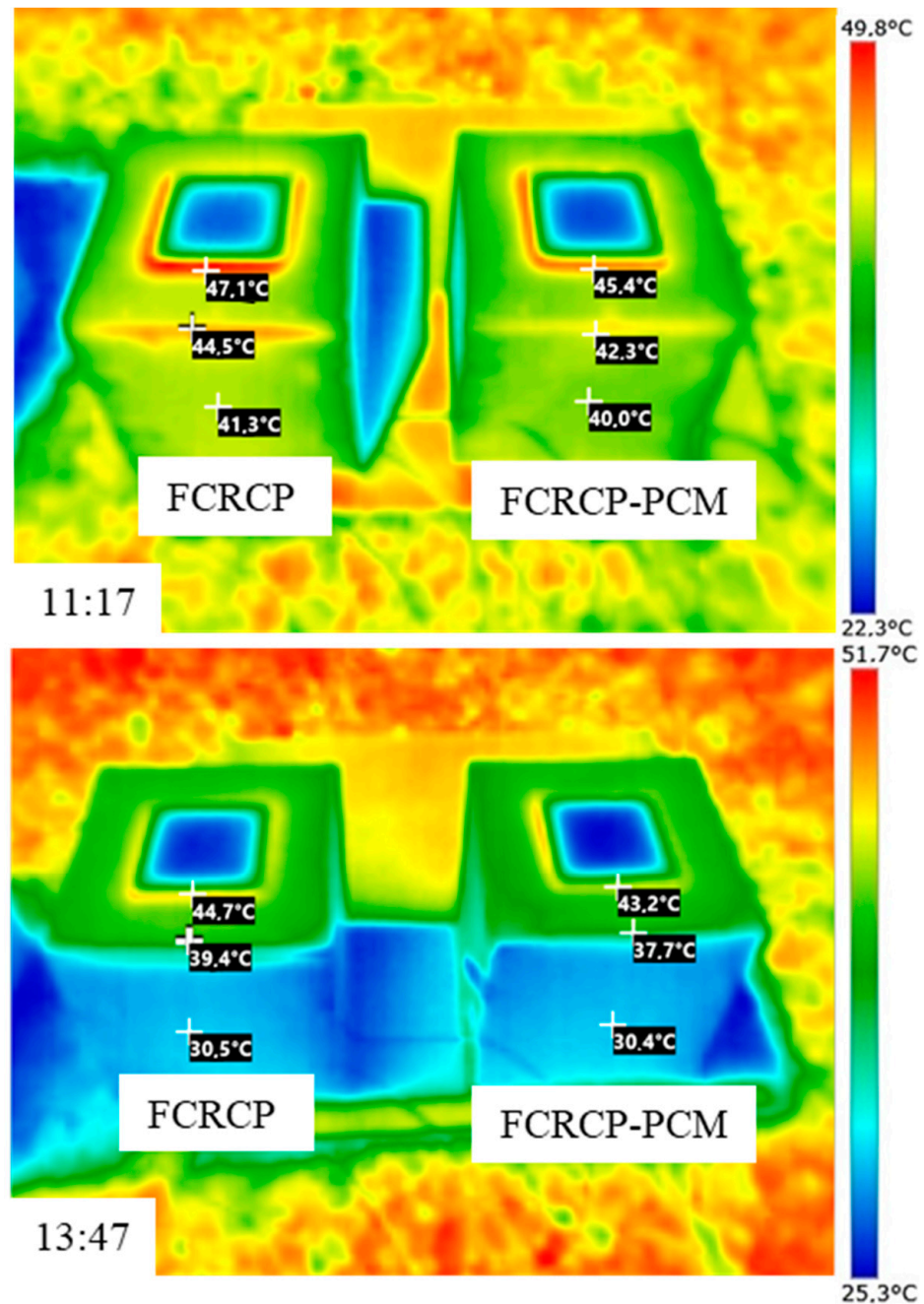


Figure 18. Thermal and real camera images of the test rooms at various hours on 28 April 2022.

4. Conclusions

To increase energy efficiency of buildings, porous composites have been used for many decades with successful results in reducing the thermal conductivity of buildings. Nonetheless, various porous composites are known to have little capacity to store thermal

energy which reduces their effectiveness in lowering the need for energy used to heat or cool the buildings. To address this, recent studies have documented favorable results when used various forms of PCMs, which are found beneficial in reducing the temperature intensity at peak hours due to their high capacity for latent heat storage. Despite this, PCMs have the potential to be leaked out of the produced porous composites when in liquid phase, which requires a specific impregnation method for their actual application. To address this and provide a more flexible melting and solidifying point, this study used a combination of Capric (CA)-Palmitic acid (PA) PCMs and impregnated into recycled concrete powder, which is known for its high content of fine-sized porosity. To evaluate the physico-mechanical, thermal and microstructural properties of the produced foamed composites, a series of tests have been conducted from which, the following conclusions can be drawn:

1. Based on the trials, the highest ratio of recycled concrete powder to PCM without leaking is found to be at about 20% (by weight). The results of DSC analysis show that the RCP/PCM composite produced this way has a latent heat capacity of 34.1 and 33.5 J/g in liquid and solid phases, with melting and solidifying temperatures of 21.62 and 19.75 °C, respectively. In addition, after about 300 cycles of liquifying and solidifying, the latent heat capacity is found to remain almost the same which shows the high cycling stability of the produced RCP/PCM composite.
2. The results of materials tests including unit weight, porosity, water absorption, all point to the lowered porosity and potentially pore network connectivity for samples produced with PCMs, compared to foams with silica sand. For instance, the impregnation of PCMs is found to reduce porosity and the capillary water absorption by 32% and 360%, respectively, when it is compared to foam samples produced with silica sand. This also causes some 44% increase in unit weight values, as well as 204% and 108% increase for compressive and flexural strength values (28-day), respectively. Despite such significant changes, the result of thermal conductivity shows only ~43% increase in the thermal conductivity values of mixes produced with PCMs, which can be associated with significantly lowered porosity values.
3. The result of SEM shows that when foams are produced with silica sand, the pores and cracks are relatively deep and often interconnected. Nonetheless, when recycled concrete powder is used, the overall content of pores is found to become slightly lowered but a high content of unconnected particles can be seen which represents a weak ITZ. After PCMs are impregnated into the recycled concrete powder, however, the pores are found to be highly disconnected and often better dispersed. With regards to the EDS test, the foams produced with silica sand are found to have the highest content of calcium. In turn, upon the inclusion of recycled concrete powder, very high content of carbon is observed in its microstructure. The reason for this can be high carbonation tendency of the produced samples. When PCMs are impregnated, however, the Ca, C and Si content is found to shift toward the mix with silica sand, pointing to the fact that the inclusion of PCMs has reduced carbonation tendency of the produced samples.
4. The result of temperature regulation performance test shows that up to -5.07 °C at the highest daily temperature in noon and $+3.67$ °C at the lowest temperature in evening is achieved in test rooms having the foams produced PCMs. It is also found that PCMs reduces the actual peak temperature time which further helps increasing the building energy efficiency in any climatic situation. This is further confirmed through the thermal camera results that showed up to 2.2 °C lower temperature on the surface of the produced rooms when PCMs are used.

The result of this study is found to be significant and point to the successful use of recycled concrete powder to host PCMs. Nonetheless, the future studies, can use alternative forms of PCMs with other hosting agents, or microencapsulation techniques to provide a comparative evaluation of impregnated PCMs and their respective impact on the actual thermo-regulative performance of buildings.

Author Contributions: Conceptualization, O.G. and T.O.; Data curation, O.G., G.H., A.U., A.S., G.K., O.Y.B. and M.S.; Formal analysis, O.G., G.H., A.U., A.S., G.K., O.Y.B., M.S. and T.O.; Investigation, G.H., A.U., A.S., G.K., O.Y.B. and M.S.; Project administration, O.G. and T.O.; Resources, O.G., G.H., A.U., A.S., G.K., O.Y.B., M.S. and T.O.; Supervision, O.G. and T.O.; Validation, M.N.; Visualization, M.N.; Writing—original draft, M.N.; Writing—review & editing, O.G., M.N. and T.O. All authors have read and agreed to the published version of the manuscript.

Funding: This research received no external funding.

Institutional Review Board Statement: Not applicable.

Informed Consent Statement: Not applicable.

Data Availability Statement: Not applicable.

Acknowledgments: The authors appreciate all the universities that supported this study.

Conflicts of Interest: The authors declare no conflict of interest.

Nomenclature

PCMs	Phase change materials
CA	Capric acid
PA	Palmitic acid
RCP	Recycled concrete powder
ITZ	interfacial transition zone
DSC	Differential scanning calorimetry
RCP/PCM	Recycled concrete powder impregnated with phase change materials
C&D	Construction and Demolition

References

1. The World Bank. Urban Development Overview: Development News, Research, Data | World Bank. Available online: <https://www.worldbank.org/en/topic/urbandevelopment/overview#1> (accessed on 1 May 2022).
2. Chowdhury, P.K.R.; Weaver, J.E.; Weber, E.M.; Lunga, D.; LeDoux, S.T.M.; Rose, A.N.; Bhaduri, B.L. Electricity consumption patterns within cities: Application of a data-driven settlement characterization method. *Int. J. Digit. Earth* **2020**, *13*, 119–135. [[CrossRef](#)]
3. Frequently Asked Questions (FAQs). U.S. Energy Information Administration (EIA). Available online: <https://www.eia.gov/tools/faqs/faq.php?id=86&t=1> (accessed on 1 May 2022).
4. Ahmad, M.R.; Chen, B.; Shah, S.F.A. Investigate the influence of expanded clay aggregate and silica fume on the properties of lightweight concrete. *Constr. Build. Mater.* **2019**, *220*, 253–266. [[CrossRef](#)]
5. Huang, Y.; Gong, L.; Shi, L.; Cao, W.; Pan, Y.; Cheng, X. Experimental investigation on the influencing factors of preparing porous fly ash-based geopolymer for insulation material. *Energy Build.* **2018**, *168*, 9–18. [[CrossRef](#)]
6. Gencil, O.; Nodehi, M.; Bayraktar, O.Y.; Kaplan, G.; Benli, A.; Gholampour, A.; Ozbakkaloglu, T. Basalt fiber-reinforced foam concrete containing silica fume: An experimental study. *Constr. Build. Mater.* **2022**, *326*, 126861. [[CrossRef](#)]
7. Nodehi, M. A comparative review on foam-based versus lightweight aggregate-based alkali-activated materials and geopolymer. *Innov. Infrastruct. Solut.* **2021**, *6*, 231. [[CrossRef](#)]
8. Gencil, O.; Bayraktar, O.Y.; Kaplan, G.; Arslan, O.; Nodehi, M.; Benli, A.; Gholampour, A.; Ozbakkaloglu, T. Lightweight foam concrete containing expanded perlite and glass sand: Physico-mechanical, durability, and insulation properties. *Constr. Build. Mater.* **2022**, *320*, 126187. [[CrossRef](#)]
9. Wu, Z.G.; Zhao, C.Y. Experimental investigations of porous materials in high temperature thermal energy storage systems. *Sol. Energy* **2011**, *85*, 1371–1380. [[CrossRef](#)]
10. Qiu, L.; Ouyang, Y.; Feng, Y.; Zhang, X. Review on micro/nano phase change materials for solar thermal applications. *Renew. Energy* **2019**, *140*, 513–538. [[CrossRef](#)]
11. Alawadhi, E.M. The design, properties, and performance of concrete masonry blocks with phase change materials. In *Eco-Efficient Masonry Bricks and Blocks*; Elsevier: Amsterdam, The Netherlands, 2015; pp. 231–248.
12. Al Shannaq, R.; Farid, M.M. Microencapsulation of phase change materials (PCMs) for thermal energy storage systems. In *Advances in Thermal Energy Storage Systems*; Elsevier: Amsterdam, The Netherlands, 2015; pp. 247–284.
13. Mäkinen, M. Introduction to phase change materials. In *Intelligent Textiles and Clothing*; Elsevier: Amsterdam, The Netherlands, 2006; pp. 21–33.

14. Cai, Y.; Zong, X.; Zhang, J.; Hu, Y.; Wei, Q.; He, G.; Wang, X.; Zhao, Y.; Fong, H. Electrospun nanofibrous mats absorbed with fatty acid eutectics as an innovative type of form-stable phase change materials for storage and retrieval of thermal energy. *Sol. Energy Mater. Sol. Cells* **2013**, *109*, 160–168. [[CrossRef](#)]
15. Hekimoğlu, G.; Nas, M.; Ouikhalfan, M.; Sari, A.; Tyagi, V.V.; Sharma, R.K.; Kurbetci, Ş.; Saleh, T.A. Silica fume/capric acid-stearic acid PCM included-cementitious composite for thermal controlling of buildings: Thermal energy storage and mechanical properties. *Energy* **2021**, *219*, 119588. [[CrossRef](#)]
16. Gencil, O.; Hekimoğlu, G.; Sari, A.; Sutcu, M.; Er, Y.; Ustaoglu, A. A novel energy-effective and carbon-emission reducing mortars with bottom ash and phase change material: Physico-mechanical and thermal energy storage characteristics. *J. Energy Storage* **2021**, *44*, 103325. [[CrossRef](#)]
17. Hekimoğlu, G.; Nas, M.; Ouikhalfan, M.; Sari, A.; Kurbetci, Ş.; Tyagi, V.V.; Sharma, R.K.; Saleh, T.A. Thermal management performance and mechanical properties of a novel cementitious composite containing fly ash/lauric acid-myristic acid as form-stable phase change material. *Constr. Build. Mater.* **2021**, *274*, 122105. [[CrossRef](#)]
18. Liu, S.; Xin, S.; Jiang, S. Study of Capric–Palmitic Acid/Clay Minerals as Form-Stable Composite Phase-Change Materials for Thermal Energy Storage. *ACS Omega* **2021**, *6*, 24650–24662. [[CrossRef](#)] [[PubMed](#)]
19. Du, W.; Fei, H.; Pan, Y.; He, Q.; Zhou, J.; Liang, X. Development of capric acid-stearic acid-palmitic acid low-eutectic phase change material with expanded graphite for thermal energy storage. *Constr. Build. Mater.* **2021**, *320*, 126309. [[CrossRef](#)]
20. Jia, W.; Wang, C.; Wang, T.; Cai, Z.; Chen, K. Preparation and performances of palmitic acid/diatomite form-stable composite phase change materials. *Int. J. Energy Res.* **2020**, *44*, 4298–4308. [[CrossRef](#)]
21. Jamekhorshid, A.; Sadrameli, S.M.; Farid, M. A review of microencapsulation methods of phase change materials (PCMs) as a thermal energy storage (TES) medium. *Renew. Sustain. Energy Rev.* **2014**, *31*, 531–542. [[CrossRef](#)]
22. Fei, H.; Wang, L.; He, Q.; Du, W.; Gu, Q.; Pan, Y. Preparation and Properties of a Composite Phase Change Energy Storage Gypsum Board Based on Capric Acid-Paraffin/Expanded Graphite. *ACS Omega* **2021**, *6*, 6144–6152. [[CrossRef](#)]
23. Horsakulthai, V. Effect of recycled concrete powder on strength, electrical resistivity, and water absorption of self-compacting mortars. *Case Stud. Constr. Mater.* **2021**, *15*, e00725. [[CrossRef](#)]
24. Environmental Protection Agency. Sustainable Management of Construction and Demolition Materials. 2022. Available online: <https://www.epa.gov/smm/sustainable-management-construction-and-demolition-materials> (accessed on 22 May 2022).
25. Rajhans, P.; Panda, S.K.; Nayak, S. Sustainable self compacting concrete from C&D waste by improving the microstructures of concrete ITZ. *Constr. Build. Mater.* **2018**, *163*, 557–570. [[CrossRef](#)]
26. Pasupathy, K.; Ramakrishnan, S.; Sanjayan, J. Influence of recycled concrete aggregate on the foam stability of aerated geopolymer concrete. *Constr. Build. Mater.* **2021**, *271*, 121850. [[CrossRef](#)]
27. Yang, D.; Liu, M.; Zhang, Z.; Yao, P.; Ma, Z. Properties and modification of sustainable foam concrete including eco-friendly recycled powder from concrete waste. *Case Stud. Constr. Mater.* **2022**, *16*, e00826. [[CrossRef](#)]
28. Caneda-Martínez, L.; Monasterio, M.; Moreno-Juez, J.; Martínez-Ramírez, S.; García, R.; Frías, M. Behaviour and Properties of Eco-Cement Pastes Elaborated with Recycled Concrete Powder from Construction and Demolition Wastes. *Materials* **2021**, *14*, 1299. [[CrossRef](#)] [[PubMed](#)]
29. Martínez, C.M.; del Bosque, I.F.S.; Medina, G.; Frías, M.; de Rojas, M.I.S. Fillers and additions from industrial waste for recycled aggregate concrete. In *The Structural Integrity of Recycled Aggregate Concrete Produced with Fillers and Pozzolans*; Elsevier: Amsterdam, The Netherlands, 2022; pp. 105–143.
30. Raj, A.; Sathyan, D.; Mini, K.M. Physical and functional characteristics of foam concrete: A review. *Constr. Build. Mater.* **2019**, *221*, 787–799. [[CrossRef](#)]
31. Abdel-Gawwad, H.A.; Mohammed, A.H.; Arif, M.A.; Shoukry, H.; Abadel, A.A.; Al-Kroom, H.; Sikora, P.; Elrahman, M.A. Role of magnesium chloride in the performance and phase composition of lead glass sludge foam. *Mater. Lett.* **2022**, *320*, 132325. [[CrossRef](#)]
32. Kastiukas, G.; Zhou, X.; Castro-Gomes, J. Development and optimisation of phase change material-impregnated lightweight aggregates for geopolymer composites made from aluminosilicate rich mud and milled glass powder. *Constr. Build. Mater.* **2016**, *110*, 201–210. [[CrossRef](#)]
33. Sakulich, A.R.; Bentz, D.P. Incorporation of phase change materials in cementitious systems via fine lightweight aggregate. *Constr. Build. Mater.* **2012**, *35*, 483–490. [[CrossRef](#)]
34. Xu, B.; Li, Z. Paraffin/diatomite composite phase change material incorporated cement-based composite for thermal energy storage. *Appl. Energy* **2013**, *105*, 229–237. [[CrossRef](#)]
35. Li, X.; Sanjayan, J.G.; Wilson, J.L. Fabrication and stability of form-stable diatomite/paraffin phase change material composites. *Energy Build.* **2014**, *76*, 284–294. [[CrossRef](#)]
36. Hunger, M.; Entrop, A.G.; Mandilaras, I.; Brouwers, H.J.H.; Founti, M. The behavior of self-compacting concrete containing micro-encapsulated Phase Change Materials. *Cem. Concr. Compos.* **2009**, *31*, 731–743. [[CrossRef](#)]
37. Nomura, T.; Okinaka, N.; Akiyama, T. Impregnation of porous material with phase change material for thermal energy storage. *Mater. Chem. Phys.* **2009**, *115*, 846–850. [[CrossRef](#)]
38. Memon, S.A.; Cui, H.Z.; Zhang, H.; Xing, F. Utilization of macro encapsulated phase change materials for the development of thermal energy storage and structural lightweight aggregate concrete. *Appl. Energy* **2015**, *139*, 43–55. [[CrossRef](#)]

39. Limbachiya, M.; Meddah, M.S.; Ouchagour, Y. Use of recycled concrete aggregate in fly-ash concrete. *Constr. Build. Mater.* **2011**, *14*, 13–18. [CrossRef]
40. Wille, K.; Naaman, A.E.; El-Tawil, S.; Parra-Montesinos, G.J. Ultra-high performance concrete and fiber reinforced concrete: Achieving strength and ductility without heat curing. *Mater. Struct. Constr.* **2012**, *45*, 309–324. [CrossRef]
41. Nodehi, M.; Nodehi, S.E. Ultra high performance concrete (UHPC): Reactive powder concrete, slurry infiltrated fiber concrete and superabsorbent polymer concrete. *Innov. Infrastruct. Solut.* **2022**, *7*, 39. [CrossRef]
42. Sari, A.; Bicer, A.; Al-Ahmed, A.; Al-Sulaiman, F.A.; Zahir, M.H.; Mohamed, S.A. Silica fume/capric acid-palmitic acid composite phase change material doped with CNTs for thermal energy storage. *Sol. Energy Mater. Sol. Cells* **2018**, *179*, 353–361. [CrossRef]
43. Liu, S.; Zhang, X.; Zhu, X.; Xin, S. A Low-Temperature Phase Change Material Based on Capric-Stearic Acid/Expanded Graphite for Thermal Energy Storage. *ACS Omega* **2021**, *6*, 17988–17998. [CrossRef] [PubMed]
44. ASTM C642; Standard Test Method for Density, Absorption, and Voids in Hardened Concrete. ASTM International: West Conshohocken, PA, USA, 2013; pp. 1–3. [CrossRef]
45. ASTM C348; Standard Test Method for Flexural Strength of Hydraulic-Cement Mortars. ASTM International: West Conshohocken, PA, USA, 1998; Volume 4, pp. 2–7. [CrossRef]
46. ASTM C 109/C 109M-02; Standard Test Method for Compressive Strength of Hydraulic Cement Mortars. ASTM International: West Conshohocken, PA, USA, 2005; Volume 4, p. 9. [CrossRef]
47. ASTM:C138/C138M-13; Standard Test Method for Density (Unit Weight), Yield, and Air Content (Gravimetric). ASTM International: West Conshohocken, PA, USA, 2013; Volume i, pp. 23–26. [CrossRef]
48. EN 1015-18; Determination of Water Absorption Coefficient due to Capillary Action of Hardened Mortar. European Standards: Brussels, Belgium, 2018. Available online: <https://www.en-standard.eu/din-en-1015-18-methods-of-test-for-mortar-for-masonry-part-18-determination-of-water-absorption-coefficient-due-to-capillary-action-of-hardened-mortar/> (accessed on 17 May 2022).
49. Gencil, O.; Yaras, A.; Hekimoğlu, G.; Ustaoglu, A.; Erdogmus, E.; Sutcu, M.; Sari, A. Cement based-thermal energy storage mortar including blast furnace slag/capric acid shape-stabilized phase change material: Physical, mechanical, thermal properties and solar thermoregulation performance. *Energy Build.* **2022**, *258*, 111849. [CrossRef]
50. Canbaz, M. The effect of high temperature on reactive powder concrete. *Constr. Build. Mater.* **2014**, *70*, 508–513. [CrossRef]
51. He, Z.; Han, X.; Zhang, M.; Yuan, Q.; Shi, J.; Zhan, P. A novel development of green UHPC containing waste concrete powder derived from construction and demolition waste. *Powder Technol.* **2022**, *398*, 117075. [CrossRef]
52. Kim, Y.-J. Quality properties of self-consolidating concrete mixed with waste concrete powder. *Constr. Build. Mater.* **2017**, *135*, 177–185. [CrossRef]
53. Sukontasukkul, P.; Uthaichotirat, P.; Sangpet, T.; Sisomphon, K.; Newlands, M.; Siripanichgorn, A.; Chindaprasirt, P. Thermal properties of lightweight concrete incorporating high contents of phase change materials. *Constr. Build. Mater.* **2019**, *207*, 431–439. [CrossRef]
54. Edwin, R.S.; Mushthofa, M.; Gruyaert, E.; de Belie, N. Quantitative analysis on porosity of reactive powder concrete based on automated analysis of back-scattered-electron images. *Cem. Concr. Compos.* **2019**, *96*, 1–10. [CrossRef]
55. Shi, C.; Li, Y.; Zhang, J.; Li, W.; Chong, L.; Xie, Z. Performance enhancement of recycled concrete aggregate—A review. *J. Clean. Prod.* **2016**, *112*, 466–472. [CrossRef]
56. Ren, P.; Li, B.; Yu, J.-G.; Ling, T.-C. Utilization of recycled concrete fines and powders to produce alkali-activated slag concrete blocks. *J. Clean. Prod.* **2020**, *267*, 122115. [CrossRef]
57. Du, Y.; Liu, P.; Quan, X.; Ma, C. Characterization and cooling effect of a novel cement-based composite phase change material. *Sol. Energy* **2020**, *208*, 573–582. [CrossRef]
58. Bi, L.; Long, G.; Ma, C.; Xie, Y. Experimental investigation on the influence of phase change materials on properties and pore structure of steam-cured mortar. *Arch. Civ. Mech. Eng.* **2021**, *21*, 11. [CrossRef]
59. Singh, M. Coal bottom ash. In *Waste and Supplementary Cementitious Materials in Concrete*; Elsevier: Amsterdam, The Netherlands, 2018; pp. 3–50.
60. Wang, H.; Wang, L.; Shen, W.; Cao, K.; Sun, L.; Wang, P.; Cui, L. Compressive Strength, Hydration and Pore Structure of Alkali-Activated Slag Mortars Integrating with Recycled Concrete Powder as Binders. *KSCE J. Civ. Eng.* **2022**, *26*, 795–805. [CrossRef]
61. Sanfeliu, S.G.; Santacruz, I.; Szczotok, A.M.; Belloc, L.M.O.; de la Torre, A.G.; Kjøniksen, A.-L. Effect of microencapsulated phase change materials on the flow behavior of cement composites. *Constr. Build. Mater.* **2019**, *202*, 353–362. [CrossRef]
62. Ratna, D. Thermal properties of thermosets. In *Thermosets*; Elsevier: Amsterdam, The Netherlands, 2012; pp. 62–91.
63. Ting, T.Z.H.; Rahman, M.E.; Lau, H.H.; Ting, M.Z.Y.; Pakrashi, V. Oil Palm Kernel Shell—A Potential Sustainable Construction Material. In *Encyclopedia of Renewable and Sustainable Materials*; Elsevier: Amsterdam, The Netherlands, 2020; pp. 137–143.
64. Qiao, L.; Li, N.; Luo, L.; He, J.; Lin, Y.; Li, J.; Yu, J.; Guo, C.; Murto, P.; Xu, X. Design of monolithic closed-cell polymer foams via controlled gas-foaming for high-performance solar-driven interfacial evaporation. *J. Mater. Chem. A* **2021**, *9*, 9692–9705. [CrossRef]
65. Wang, K.; Ren, L.; Yang, L. Excellent Carbonation Behavior of Rankinite Prepared by Calcining the C-S-H: Potential Recycling of Waste Concrete Powders for Prefabricated Building Products. *Materials* **2018**, *11*, 1474. [CrossRef]
66. Liu, Z.; Hu, W.; Hou, L.; Deng, D. Effect of carbonation on physical sulfate attack on concrete by Na₂SO₄. *Constr. Build. Mater.* **2018**, *193*, 211–220. [CrossRef]

67. Belessiotis, V.; Kalogirou, S.; Delyannis, E. Solar Distillation—Solar Stills. In *Thermal Solar Desalination*; Elsevier: Amsterdam, The Netherlands, 2016; pp. 103–190.
68. Page, J.K. Radiation data. In *Solar Energy Conversion II*; Elsevier: Amsterdam, The Netherlands, 1981; pp. 23–35.
69. Gencil, O.; Ustaoglu, A.; Benli, A.; Hekimoğlu, G.; Sarı, A.; Erdogmus, E.; Sutcu, M.; Kaplan, G.; Bayraktar, O.Y. Investigation of physico-mechanical, thermal properties and solar thermoregulation performance of shape-stable attapulgite based composite phase change material in foam concrete. *Sol. Energy* **2022**, *236*, 51–62. [[CrossRef](#)]